

Human Neutrophil Elastase-Mediated Cleavage Sites of MMP-9 and TIMP-1: Implications to Cystic Fibrosis Proteolytic Dysfunction

Patricia L Jackson,^{1,2} Xin Xu,^{1,2} Landon Wilson,³ Nathaniel M Weathington,¹ John Paul Clancy,^{4,5} James Edwin Blalock,^{1,2,5} and Amit Gaggar^{1,2,5,6}

¹Department of Medicine, ²Department of Physiology and Biophysics, ³Comprehensive Cancer Center, ⁴Department of Pediatrics, and ⁵Gregory Fleming James Cystic Fibrosis Center, University of Alabama at Birmingham, Birmingham, Alabama, United States of America; ⁶Birmingham VA Medical Center, Birmingham, Alabama, United States of America

Cystic fibrosis (CF) is a lethal genetic disorder characterized by airway remodeling and inflammation, leading to premature death. Recent evidence suggests the importance of protease activity in CF pathogenesis. One prominent protease, matrix metalloprotease (MMP)-9, demonstrates increased activity in CF individuals undergoing acute pulmonary exacerbation. This is thought to be mediated by both direct MMP-9 activation and the degradation of its natural inhibitor, tissue inhibitor of metalloprotease-1 (TIMP-1). To examine if this relationship exists in nonexacerbating CF individuals, we examined protease activity in sputum from these individuals compared with nondisease controls. We demonstrated increased gelatinolytic activity in CF sputum. These samples had elevated human neutrophil elastase (HNE) levels which correlated with an increased MMP-9/TIMP-1 ratio. To determine if HNE could discretely cleave and activate MMP-9, these enzymes were coinubated and two specific cleavage sites, between Valine³⁸ and Alanine³⁹, and between Alanine³⁹ and glutamic acid⁴⁰ were observed. These sites corresponded with appropriate molecular weight for the activated MMP-9 isoform in CF sputum. Using N-terminal sequencing of cleavage fragments obtained with TIMP-1 incubation with HNE, we confirmed the TIMP-1 cleavage site for HNE is at Valine⁶⁹-Cysteine⁷⁰. We also show for the first time that human neutrophils were capable of degrading TIMP-1 *ex vivo* and that a 16 kDa TIMP-1 fragment was identified in CF sputum, consistent with the expected cleavage of TIMP-1 by HNE. These results demonstrate increased MMP-9 activity in stable CF lung disease, and the presence of specific protease products in CF sputum highlights that HNE-mediated activity plays a role in this dysregulation.

© 2010 The Feinstein Institute for Medical Research, www.feinsteininstitute.org

Online address: <http://www.molmed.org>

doi: 10.2119/molmed.2009.00109

INTRODUCTION

Recent models of airway inflammation indicate that protease:antiprotease imbalance is a prime contributor in the development of pulmonary diseases, with detrimental effects on resolution of inflammation and remodeling of the pulmonary architecture (1,2). Alpha-1 antitrypsin deficiency is a classic example of this process, with unchecked and unrelenting pulmonary protease activity producing emphysema and premature pulmonary failure (3). The dysregulation

of proteases with antiproteases have been characterized in a variety of other pulmonary conditions including chronic obstructive pulmonary disease (COPD) and asthma (4,5).

Cystic fibrosis (CF) is another lung disease in which unchecked protease activity has been hypothesized to damage the airway architecture and contribute to progressive bronchiectasis (6,7). Human neutrophil elastase (HNE) is a well described serine protease that has been shown to be a biomarker of pulmonary inflammation

in both α -1 antitrypsin deficiency and CF (3,8). Dysregulation of HNE propagates inflammation and is believed to disrupt the pulmonary architecture through damage of structural proteins in both diseases (3,9). Further evidence points to an important role of HNE in other pulmonary conditions and to significant immunologic effects of its dysregulated activity (10–12).

Another family of proteases increasingly well characterized in chronic inflammatory lung diseases is the matrix metalloprotease family (MMPs) (13). MMPs perform numerous biologic functions, including: degradation of matrix components and remodeling of tissues; release of cytokines, growth factors and chemokines; and modulation of cell mobility and migration (14–16).

MMPs are regulated at the level of transcription, translation and post-

Address correspondence and reprint requests to Amit Gaggar or Patricia Jackson, 1918 University Boulevard, MCLM 898, Birmingham, AL 35294. Phone: 205-934-6439 (A Gaggar), 205-934-2622 (P Jackson); Fax: 205-934-1721; E-mail: agaggar@uab.edu (A Gaggar), plj@uab.edu (P Jackson).

Submitted August 11, 2009; Accepted for publication January 21, 2010; Epub (www.molmed.org) ahead of print January 22, 2010.

translational modification (14). In addition to release of MMPs into the extracellular environment, these proteases must have their pro-domain cleaved to generate enzymatic activity (15). While *in vitro* mechanisms have been described for MMP activation (detergents, mercury-based compounds) (17), *in vivo* activation predominately centers on protease-based activation. Specific serine proteases (that is, trypsin) have been well characterized as MMP activators (18). In addition, other MMPs also may serve as potent activators (19,20). MMPs are unique proteases which can be activated by a variety of proteases and have even been shown to autocatalyze zymogen once activated.

Perhaps the best recognized mechanism of MMP regulation is through the binding of small, specific protein inhibitors (tissue inhibitor of metalloproteases [TIMPs]) to the active site of the MMP (21). Data suggest that dysregulated cellular production, secretion and activation of MMPs, and/or dysfunction of their inhibitors are involved in pathologic conditions within the lung parenchyma. Animal studies, in addition to human studies in adults, support a role for MMPs and an imbalance between MMPs and their inhibitors in the pathogenesis of several well-recognized pulmonary disorders including COPD and asthma (22,23).

Recently, our group has described the specific MMP isoform profile (MMP-8, MMP-9, MMP-11 and MMP-12) identified in the sputum of CF individuals undergoing acute pulmonary exacerbation (APE) (24). We further described an increase in MMP-9 activity with a concomitant decrease of the presence of a prominent natural inhibitor of MMP-9 in these specimens, TIMP-1. This imbalance was thought to be, in part, due to a mechanism of MMP-9 activation and TIMP-1 degradation via HNE. While these findings have shed light into a unique pathway of protease potentiation in clinical disease, it is unknown if this proteolytic dysregulation is seen in CF patients who are not undergoing APE.

In this study, we demonstrate that there is elevated HNE activity in non-

exacerbating CF patients and that there is notable correlation between MMP-9/TIMP-1 ratio and increased HNE activity in these clinically stable individuals. We then determine the specific cleavage sites for HNE for MMP-9 and demonstrate the presence of a TIMP-1 cleavage fragment in CF sputum whose size is consistent with that seen with HNE-mediated cleavage of TIMP-1 *in vitro*. These findings demonstrate important mechanisms of increased MMP-9 proteolytic activity present *in vivo* in CF lung disease. These findings also highlight that, even in CF individuals without APE, there is notable MMP-9 and HNE activity present in airway secretions. Finally, these findings underscore important, clinically relevant regulatory relationships between these molecules and may have therapeutic implications in CF lung disease.

MATERIALS AND METHODS

Patient Populations

Sputum samples from CF outpatients and normal control individuals were collected after approval by the University of Alabama at Birmingham Institutional Review Board. Basic demographic data were collected for both populations. Lung function, genotype and microbiologic data were collected for CF individuals only. Sputum samples were expectorated spontaneously for CF individuals and induced via hypertonic saline for normal individuals.

Materials

Recombinant TIMP-1, MMP-9 and IL-8 were purchased from R & D Systems (Minneapolis, MN, USA). Recombinant HNE and HNE specific inhibitor was purchased from Calbiochem (San Diego, CA, USA).

Sputum and Endotracheal Aspirate Processing

Once collected, the sputum was diluted 1:2 with 0.9% normal saline and centrifuged at 200g for 10 min with separation of pellet from supernatant. The

supernatant was collected, protein concentration was measured, and then separate aliquots were saved for measurements (-80°C).

Zymography

Porcine skin gelatin (Sigma, St. Louis, MO, USA) at 1 mg/mL was added to a 7.5% SDS polyacrylamide solution before casting. Biologic samples were aliquoted and diluted in nonreducing sample buffer, and 16 μg of sample were added to each lane. All samples were electrophoresed at 12 mA for 1 h. Following electrophoresis, gels were washed in 2.5% Triton X-100 for 1 h at 4°C , then incubated in 50 mM Tris-Cl for 16 h at 37°C . Gels were stained in 0.05% Coomassie blue for 30 min and subsequently destained for 2 h.

MMP-9 Activity Assay

Briefly, MMP-9 specific ELISA-based activity assays were used to quantify specific MMP activity (R & D Systems). Samples were diluted to fit manufacturer's sensitivity for individual kits (0–16 ng/mL). Both samples and recombinant enzyme standards were prepared and incubated for 2 h at room temperature in 96-well plates coated with monoclonal antibody for MMP-9 (MAB 911) of interest. After incubation, samples and standards were activated with 1 mM aminophenylmercuric acetate (APMA), a chemical activator of MMPs, and further incubated for 2 h at 37°C . After incubation, a fluorogenic substrate (Fluor-Pro-Leu-Gly-Leu-Ala-Arg-NH₂) was placed in each well and the plate was incubated at 37°C for 18 h. The plate was then read on a SpectraMax Gemini spectrophotometer (Molecular Devices, Sunnyvale, CA, USA) with excitation and emission wavelengths of 320 and 405, respectively, and data was quantified using standard curves provided with the kits.

TIMP-1 Enzyme-Linked Immunosorbent Assay (ELISA)

For the studies of TIMP-1, samples were diluted to fit manufacturer's sensitivity for ELISA (0–10 ng/mL). Both sam-

ples and recombinant TIMP-1 standards were prepared and incubated for 2 h at room temperature in 96-well plates coated with TIMP-1 monoclonal antibodies. Bound TIMP-1 was then treated with a horseradish peroxidase-based secondary antibody for 1 h. A colorimetric substrate (hydrogen peroxide and chromagen) was placed in each well and color change was assessed after 30 min. Color changes were quantified on a colorimeter (Bio-Rad, Hercules, CA, USA) via standard curves provided with the kits.

Human Neutrophil Elastase (HNE)

Assays

Briefly, HNE-specific ELISA activity kits were used to quantify HNE concentrations in clinical samples (Calbiochem). Samples were diluted to fit manufacturer's kit specificity (0–20 ng/mL). Both samples and recombinant HNE standards were prepared and incubated for 2 h at room temperature in 96-well plates coated with a monoclonal antibody for HNE. A fluorogenic substrate (MeOSuc-Ala-Ala-Pro-Val-AMC) was then added and the plate was incubated for 2 h. Finally, the plate was read on a Spectra-Max Gemini spectrophotometer (Molecular Devices) with excitation and emission wavelength of 360 and 460, respectively, and data was quantified using standard curves provided with the kits.

MMP-9 and HNE Coincubation and Protein Blot

MMP-9 (2.0 µg; R & D Systems) appropriately diluted in 50 µL dH₂O was mixed with equal volumes of 2.0 µg HNE (Calbiochem) and incubated at 4°C for 15–60 min. The reaction solution was filtered by using Ultracel YM membrane (YM-10, Millipore, Billerica, MA, USA) at 4°C. The cleavage fragments collected from filter were run on 7.5% nonreducing SDS/polyacrylamide gel. The gel was then stained with 0.05% coomassie blue for 1 h and destained with a solution containing methanol/acetic acid/water (45:10:45) until the bands appeared on a clear background. The different sizes of bands were cut for sequence analysis.

Peripheral Blood Human PMN Isolation

Peripheral blood was layered onto a dual gradient of Histo-Paque 11191 (bottom) and Histo-Paque 11077 (top) and spun at 800g for 30 min at room temperature. The neutrophil layer was defined at the location directly above the red blood cell pellet. Cells were aspirated and washed in PBS. The cells were resuspended in ACK red cell lysis buffer for 15 min and washed in PBS. The cells were resuspended in the desired solution, cytospun and differentially stained to check for purity (>95% PMNs).

TIMP-1 and HNE Coincubation

Recombinant human TIMP-1 (100 µg/mL, 28 kDa) was incubated with recombinant HNE (50 µg/mL, 27 kDa) over 2 h at 37°C. Samples were then run on a 10% SDS-PAGE and stained with 0.05% coomassie blue and subsequently destained with a solution containing methanol/acetic acid/water (45:10:45) until the bands appeared on a clear background.

TIMP-1 and PMN Lysate Coincubation

Isolated primary human PMNs (2.5 × 10⁵ cells) were initially activated with 50 ng/mL of IL-8 for 1 h and then lysed via freeze-thaw. HNE concentration of lysate was then measured (150 ng/mL) and then this lysate was incubated with either an HNE-specific inhibitor or DMSO (vehicle) overnight at 40°C. Thereafter, 1 µg of TIMP-1 was added and incubation continued for 8 and 24 h at 37°C water bath. After that, the reaction solution was loaded on 15% SDS-PAGE gel for electrophoresis.

Western Blot

Samples were electrophoresed through SDS-PAGE via nonreducing conditions. Membranes were blocked with Tris buffer (pH 7.4) containing 5% powdered milk for 1 h. Once washed, the samples were incubated with polyclonal TIMP-1 primary antibody (Chemicon [Millipore], Temecula, CA, USA) overnight at 4°C. After incubation, samples were washed

and incubated with secondary antibody (IgG goat-antirabbit from Dako, Glostrup, Denmark), conjugated with horseradish peroxidase at dilution of 1:5000 for 1 h. Immunoblots then were developed utilizing Pico ECL reagent (Thermo Scientific Rockford, IL, USA).

N-Terminal Sequencing for TIMP-1 Fragment

Tandem mass spectral analyses were performed with a q-TOF-2 mass spectrometer (Micromass, Manchester, UK) using electrospray ionization. Samples had undergone a 16-h tryptic digest at 37°C. The resulting peptides were purified using Zip Tips (Millipore, Billerica, MA, USA) to concentrate and desalt the samples. The samples then were analyzed by LC-MS-MS. Liquid chromatography was performed using an LC Packing Ultimate LC, Switchos microcolumn switching unit and Famos autosampler (LC Packing, San Francisco, CA, USA). The samples were concentrated on a 300 µm i.d. C18 precolumn at a flow rate of 10 µL/min with 0.1% formic acid and was then flushed onto a 75 µm i.d. C18 column at 200 nL/min with a gradient of 5%–100% (0.1% formic acid) in 30 min. The nano-LC interface was used to transfer the liquid chromatography eluent into the mass spectrometer. The q-TOF was operated in the automatic switching mode whereby multiply charged ions were subjected to MS-MS if their intensities rose above six counts. The tandem mass spectra were processed with the Mass Lynx MaxEnt 3 software.

Nano-LC Tandem Mass Spectrometry for MMP-9/HNE Cleavage Site

An aliquot (5–10 µL) of each digest was loaded onto a 5 mm × 100 µm i.d. C₁₈ reverse-phase cartridge at 2 µL/min using a PAL robot (Leap Technologies, Carrboro, NC, USA). After washing the cartridge for 5 min with 0.1% formic acid in ddH₂O, the bound peptides were flushed onto a 22 cm × 100 µm i.d. C₁₈ reverse-phase pulled tip analytical column with a 25-min linear 5–50% acetonitrile gradient in 0.1% formic acid at

500 nL/min using an Eksigent nanopump (Eksigent Technologies, Dublin, CA, USA). The column was washed with 90% acetonitrile-0.1% formic acid for 15 min and then re-equilibrated with 5% acetonitrile-0.1% formic acid for 24 min. The eluted peptides were passed directly from the tip into a modified MicroIon-Spray interface of an Applied Biosystems-MDS-Sciex (Concorde, Ontario, Canada) 4000 Qtrap mass spectrometer.

Eluted peptides were subjected to a survey MS scan to determine the top three most intense ions. A second scan (the enhanced resolution scan) determined the charge state of the selected ions. Finally, enhanced product ion scans were carried out to obtain the tandem mass spectrum of the selected parent ions (with the declustering potential raised to 100 V) over the range from m/z 400-1500. Spectra are centroided and deisotoped by Analyst Software, version 1.42 (Applied Biosystems). These tandem mass spectrometry data are processed to provide protein identifications using an in-house MASCOT search engine (Matrix Science) against a known enzyme cleavage search algorithm.

Statistical Analysis

Descriptive statistics including mean and standard error of the mean (SEM) were determined for all continuous data. Nonparametric testing was used to compare populations in this study via the exact Wilcoxon rank sum test for unpaired data. Spearman correlation coefficient was used for relationship between MMP-9/TIMP-1 ratio and HNE.

RESULTS

Clinically stable, nonexacerbating CF individuals ($n = 9$) were examined and compared with a population of nondisease controls ($n = 5$). The CF individuals had an average age of 26.1 years (± 2.6) and were 33% male/67% female versus an average age of 32.0 (± 2.9) and 40% male/60% female in nondisease control. 22% of CF individuals were $\Delta F508$ homozygous, while the remainder of the individuals were $\Delta F508$ heterozygous.

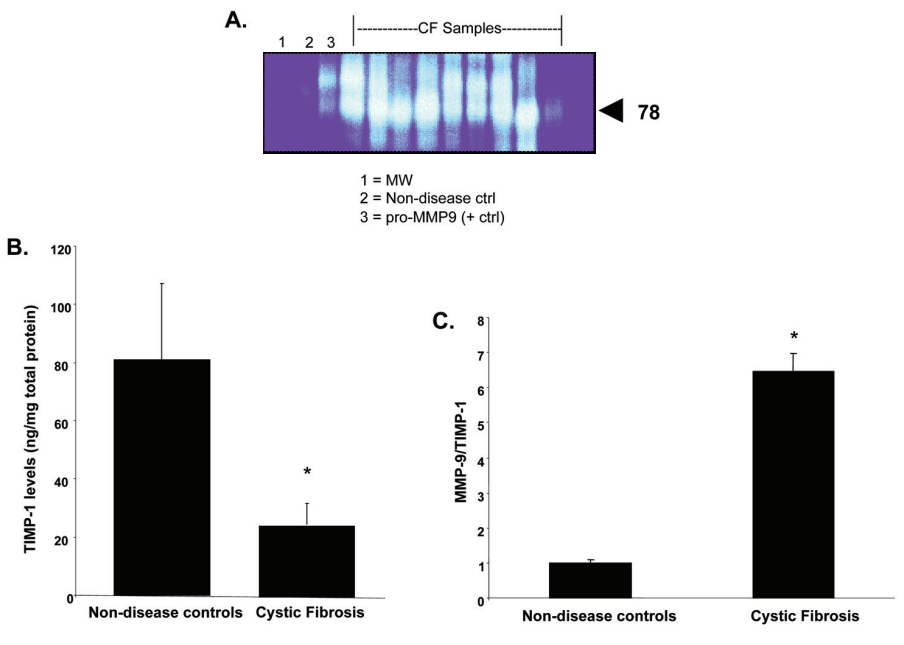


Figure 1. (A) CF patients demonstrate elevated gelatinase activity: CF clinical samples on gelatin zymogram with increased 78 kDa band. Each lane represents a separate patient. (B) CF patients have reduced TIMP-1 levels: Sputum from CF patients ($n = 9$) are measured via ELISA compared with normal nondisease controls ($n = 5$), $*P < 0.05$. (C) CF patients have an elevated MMP-9/TIMP-1 ratio: Sputum from CF patients ($n = 9$) MMP-9/TIMP-1 levels are compared with normal nondisease controls ($n = 5$), $*P < 0.01$.

Most of the CF individuals were pseudomonas positive via sputum culture (89%) and 33% were also staph aureus positive. None of the patients were *B. cepacia* positive. The average FEV1 was 62.4% of predicted for age-matched normal controls (± 6.0) and the average FVC was 74.9% of predicted for age-matched normal controls (± 4.7). None of these patients had demonstrated a significant decline in lung function or change in baseline pulmonary symptoms compared with their previous clinic visits.

To first determine if stable, nonexacerbating CF patient samples demonstrated increased proteolytic activity, we first examined them via gelatin zymography. These samples demonstrated increased activity (78 kDa) when compared with normal control individuals (Figure 1A). We further characterized the MMP profile in this population, demonstrating increased expression of MMP-9 via Western blots (data not shown). TIMP-1, a natural inhibitor of MMP-9, also was

quantified and found to be at significantly lower levels when compared with normal controls (Figure 1B). The ratio of MMP-9/TIMP-1 was significantly higher in the stable CF outpatient population when compared with nondisease controls (Figure 1C).

These results parallel the findings of significantly increased HNE activity in CF samples (Figure 2A), leading to the possibility that a relationship may exist between these molecules in CF individuals without APE. When the HNE activity in these samples was compared with their MMP-9/TIMP-1 ratio, we find a significant correlation coefficient (R^2) of 0.65 (Figure 2B, $P < 0.05$). These results demonstrate that a relationship of protease dysregulation involving these mediators exists in individuals with clinically stable CF lung disease.

Previously, we have demonstrated the capability of HNE to cleave and activate pro-MMP-9 and degrade TIMP-1 *in vitro*, hypothesizing that this prote-

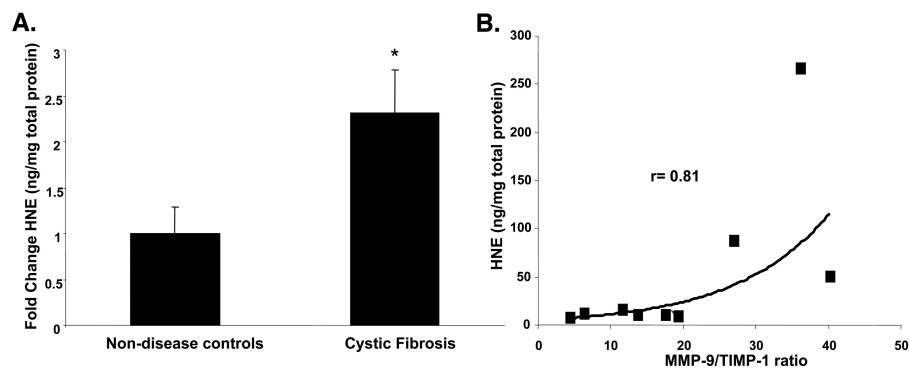


Figure 2. (A) CF patients demonstrate increased HNE activity: Sputum from CF patients ($n = 9$) are measured for HNE activity and then normalized to normal nondisease controls ($n = 5$), $*P < 0.05$. (B) MMP-9/TIMP-1 ratio correlates with HNE concentration in CF patients: MMP-9/TIMP-1 ratio and HNE concentration demonstrates an r value of 0.81 ($P < 0.05$) in CF specimens ($n = 9$).

olytic dysregulation is likely operative in CF lung disease. The determination of the site of action of HNE on the molecules may, therefore, have important implications to CF-specific therapeutics. To determine the HNE-specific proteolytic site(s) on MMP-9 to induce its activation, we incubated pro-MMP-9 with HNE *in vitro* and examined cleavage over time. A major band was seen with the coincubation at various time points (Figure 3A), consistent with a major band seen in CF sputum (see Figure 1A). Utilizing mass spectrometry to examine the incubated samples, the specific cleavage sites for HNE were determined as Val³⁸-Ala³⁹ and Ala³⁹-Glu⁴⁰ (Figure 3B).

Previously, Nagase and colleagues had demonstrated that HNE specifically cleaved TIMP-1 at Val⁶⁹, leading to a 16 kDa fragment (25,26). To verify this specific cleavage site of TIMP-1, we incubated recombinant TIMP-1 with HNE for 2 h. We noted a depletion of TIMP-1 with the emergence of the expected 16 kDa band (Figure 4A). This band was then cut from the gel and sequenced (Figure 4B). This fragment was found to be cleaved from TIMP-1 and showed a cleavage site between Val⁶⁹ and Cys⁷⁰, confirming a previous finding by Nagase *et al.* We then demonstrated that TIMP-1 can be degraded effectively from pri-

mary human PMNs and that this degradation can be rescued by the concomitant administration of an HNE-specific inhibitor (Figure 4C). These 24-h results were similar to results observed at 8 h of coincubation (data not shown). To our knowledge, however, the presence of this predicted fragment has not been demonstrated in clinical disease samples. Utilizing an antibody for TIMP-1, we demonstrate the presence of a 16 kDa TIMP-1 fragment in CF specimens (Figure 4D),

consistent with HNE-mediated degradation of TIMP-1.

DISCUSSION

Our results demonstrate that in sputum from stable, nonexacerbating CF patients, there are increased levels of both HNE and MMP-9 activity. Paralleling data described previously (24,27), we show a relationship between increased HNE activity with MMP-9 and TIMP-1 in stable CF outpatients, with a statistically significant r value of 0.81. These findings suggest that this pathway of proteolytic dysregulation is operative even in CF individuals during basal disease, underscoring the importance of unrelenting HNE activity.

As previously mentioned, HNE is a member of the serine protease family which targets a variety of substrates that may modulate airway inflammatory responses through various mechanisms. HNE has also been well characterized as a marker of airway inflammation in CF lung disease (28). Recently, HNE has also been shown to have activating effects on two proteases with implications in airway inflammation, MMP-2 and cathepsin B (29).

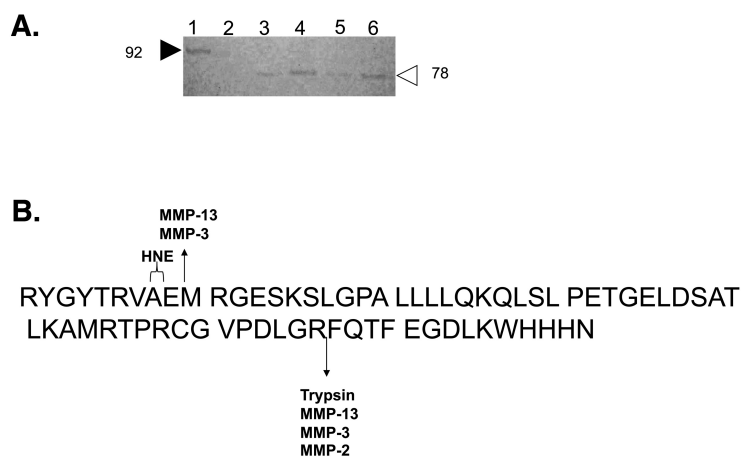


Figure 3. (A) HNE cleaves MMP-9 and produces a specific fragment: Coomassie blue stain of recombinant human MMP-9 (2 μ g) (lane 1) with HNE (2 μ g) (lane 2) at 15 min (lane 3), 30 min (lane 4), 45 min (lane 5) and 60 min (lane 6) demonstrated the presence of a 78 kDa isoform. (B) Residues of prodomain of MMP-9 cleaved by HNE: Arrows indicate other protease cleavage sites leading to activation. The two residues we found to be cleaved by HNE are also shown.

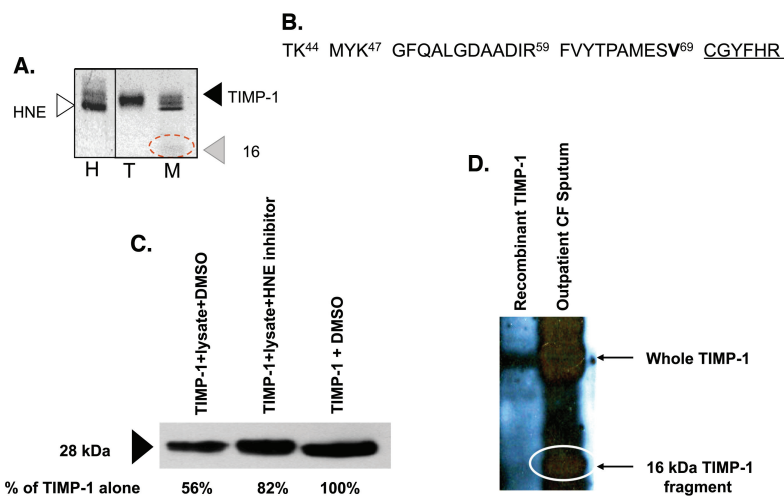


Figure 4. (A) HNE degrades TIMP-1 and produces a specific fragment: Coomassie blue stain of recombinant human TIMP-1 (100 μ g/mL, 28 kDa black arrow) incubated with recombinant HNE (50 μ g/mL, 27 kDa white arrow) for 2 h (Lane M). Lane H = HNE alone (2 h, 37°C), Lane T = TIMP-1 alone (2 h, 37°C). (B) N-terminal sequencing determines HNE-specific cleavage site of TIMP-1: 16 kDa fragment from Figure 4a was excised and underwent trypsin digestion. Trypsin-cleavage sites (noted by superscripts) were aligned; a cleavage site was found which did not correspond to trypsin specificity (underlined), corresponding to Val⁶⁹ on the TIMP-1 sequence. (C) TIMP-1 cleavage by PMN lysates is rescued by HNE inhibitor: 1 μ g of TIMP-1 was incubated with a PMN lysate, PMN lysate + elastase inhibitor (500 fold molar excess), or DMSO (elastase vehicle) for 24 h. Densitometry and band imaging was performed utilizing BioRad Chemidoc XRS system. PMN lysate decreased TIMP-1 expression to 56% of control but HNE inhibitor increases this to 82% of control TIMP-1 band. (D) TIMP-1 fragment is present in CF sputum: Western blot (12% SDS nonreduced gel) demonstrates a 28 kDa TIMP-1 band in both TIMP-1 std (20 ng/mL) and in a pooled CF sputum sample ($n = 9$). In addition, a 16 kDa TIMP-1 band is identified in the pooled CF sputum sample (white circle).

HNE demonstrates well characterized catalytic and inhibitory regions. HNE normally cleaves peptide bonds in which the P1 residue is a small alkyl group. Substrate specificity also is affected by residues P4-P2' around the scissile bond, and the specificity of HNE for these sites has been demonstrated previously (30). The locations of the cleavage sites of both MMP-9 and TIMP-1 conform to the substrate specificity of HNE.

We have determined the HNE cleavage site of the prodomain of MMP-9. In our studies, we see a peptide which corresponds to cleavage on the c-terminal side of Val³⁸ and a peptide which corresponds to cleavage on the c-terminal side of Ala³⁹. Both residues are preferred residues in the P1 site of HNE and the shift from Ala³⁹ to Val³⁸ would allow for

the P1-P3 site requirements of HNE to be satisfied. These sites are to the N-terminal side of the previously identified MMP-13 and MMP-3 cleavage site at Glu⁴⁰-Met⁴¹ (31). From the x-ray structure of MMP-9 (IRJ from RCSB protein structure database) we can see that these residues are part of a flexible loop region (due to the flexibility, all residues in the loop did not give sufficient density to allow for structure). The flexibility of the loop as well as its placement on the outer surface of the molecule means that residues in the loop are not sterically hindered and thus are very accessible to cleavage by HNE. Cleavage at this site removes the first α -helix (residues Asp⁴¹ to Arg⁵¹). This would correspond to the 86 kDa form described as inactive by Lee (31). As this site is past the glycosylation site at N¹⁸,

the exact weight loss is difficult to quantify by gel. We believe that cleavage at this site allows the second α -helix (residue Gly⁶⁷ to Leu⁷⁸) to "swing open," exposing the catalytic site of MMP-9 (Figure 5A). This would mean that the cysteine switch peptide could be removed from the active site Zn allowing the enzyme to become active. This would be compatible with earlier work showing that in the presence of SDS the enzyme gains activity (32), likely due to a similar type of conformational change as described here. MMP-9 then likely undergoes autocleavage of the remaining prodomain to give the 78 kDa active protein. This matches the data from our clinical samples (see Figure 1A) and our enzyme coin incubations (see Figure 3A). In our experiments, we were unable to distinguish the autocleavage at Phe⁸⁹ from the trypsin cleavage performed as part of the N-terminal sequencing procedure.

Utilizing N-terminal sequencing, we confirmed a consistent cleavage site at Val⁶⁹ (Figure 5B). The location of this specific cleavage site had been demonstrated previously by Nagase and colleagues (25,26). We also demonstrate primary human PMNs have the capability to degrade TIMP-1 and that this effect is mediated by HNE activity. Finally, for the first time, we demonstrate this predicted TIMP-1 cleavage fragment is present in clinical disease specimens, highlighting that this process occurs in CF lung disease.

These results strongly suggest the importance of the regulatory relationship between HNE with MMP-9 and TIMP-1 in stable, non-APE CF patients. This protease dysregulation underscores the ongoing airway remodeling and augmentation of inflammation seen in CF patients when clinically stable. In addition, unmitigated MMP-9 activity in the airways has a diverse group of effects, which may augment CF-related pathophysiology (Figure 6). This evidence highlights the importance of consideration of aggressive antiprotease therapy even in those individuals who are not undergoing frequent disease exacerbations.

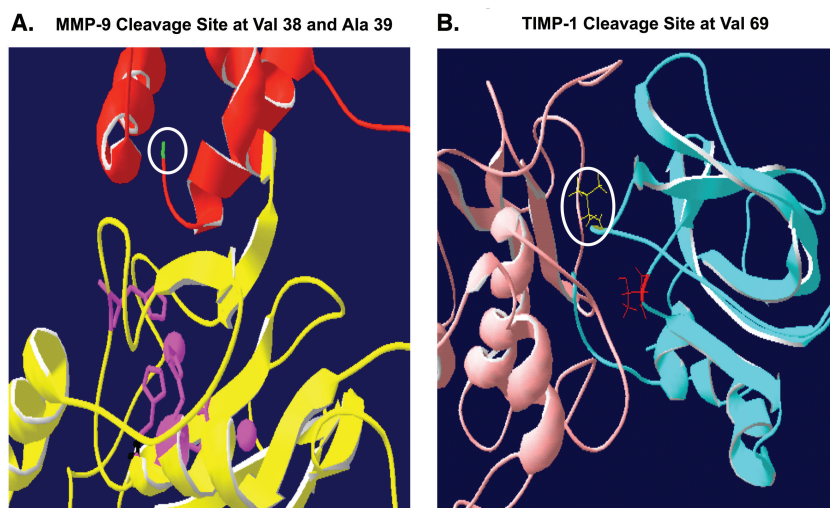


Figure 5. (A) MMP-9 Crystal Structure (RCSB structure 1R3J): The red motif represents the MMP-9 prodomain, while the yellow region represents the remainder of MMP-9 molecule. The purple region represents the catalytic site. The green residue (with white circle) shows the HNE cleavage site (Val³⁸-Ala³⁹ and Ala³⁹-Glu⁴⁰) as determined via mass spectrometry. (B) MMP-3 interaction with TIMP-1 (RCSB 1009): While the crystal structure for MMP-9/TIMP-1 interaction is not completely known, it is thought to be similar to MMP-3/TIMP-1 interaction. The pink colored molecule is MMP-3 and the light blue colored molecule is TIMP-1. The red amino acid is Thr⁶⁸, an important amino acid in TIMP-1 recognition of MMPs. HNE cleavage site for TIMP-1 is Val⁶⁹ (yellow, with white circle) as determined via N-terminal sequencing of TIMP cleavage products.

The determination of the HNE-specific cleavage site of MMP-9, confirmation of the HNE-specific TIMP-1 cleavage site, and evidence demonstrating this mechanism of MMP-9 activation is operative in CF may have implications to disease-specific therapeutics. These may include an increased interest in HNE inhibition in CF individuals to mitigate this mechanism of protease potentiation *in vivo*. Another potential application of this research may lead to the development of “designer molecules” with site specific mutations of TIMP-1 degradation in an HNE-rich environment (33). The development of novel therapeutics may lead to a restoration of the balance of MMP-9 and TIMP-1 levels in CF lung disease.

ACKNOWLEDGMENTS

The authors would like to thank Marion Kirk for his efforts in sequencing TIMP-1 fragments. We also would like to thank Uros Djekic for his contribution to this manuscript. We would like to thank

Heather Young and Ginger Reeves for their assistance in obtaining clinical specimens. We also appreciate ongoing support from the UAB Lung Health Center.

AG is funded through the UAB CIFA Award and the Cystic Fibrosis Foundation (GAGGAR07A0). JPC is funded through The Thrasher Award. JEB is funded through the Cystic Fibrosis Foundation (R464-CR02) and NIH (HL07783, HL090999 and HL087824). Resources for these studies were provided by the UAB CF Research and Translation Core Center (P30DK072482). Purchase of the mass spectrometers in the Mass Spectrometry Shared Facility came from funds provided by the NCCR Shared Instrumentation grants S10 RR06487 (PE-Sciex API 3), S10 RR11329 (Perceptive Biosystems Voyager Elite MALDI-TOF), S10 RR13795 plus UAB Health Services Foundation General Endowment Fund (Waters/Micromass Q-TOF and Applied Biosystems DE-Pro MALDI-TOF), S10 RR19231 (Applied Biosystems 4000 Qtrap). In addition, funds for instrumentation for pro-

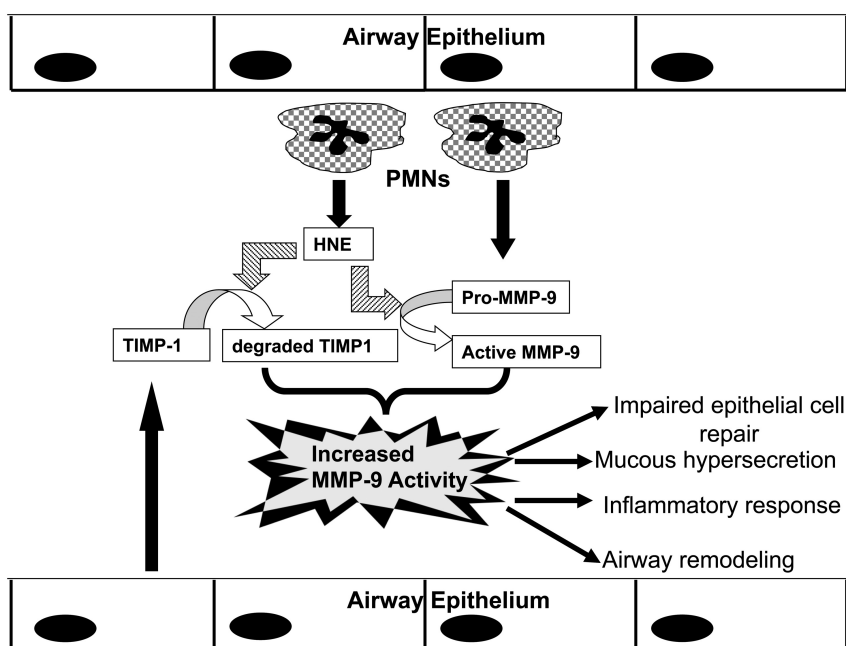


Figure 6. Increased MMP-9 activity augments potential mechanisms of CF-related pathology: Ongoing dysregulation of MMP-9 activity in CF airways impacts various aspects of CF related pathophysiology including airway remodeling, epithelial cell damage, increased mucous production and augmentation of inflammatory response.

cessing of proteomics samples were provided by NCCR Shared Instrumentation grant S10 RR16849 (HK). Funds for the operation of the Mass Spectrometry Shared Facility came in part from the UAB Comprehensive Cancer Center Core Support Grant (P30 CA13148).

DISCLOSURE

This project was supported in part by grants from the NHLBI and NIDDK. The content is solely the responsibility of the authors and does not necessarily represent the official views of the NIH.

REFERENCES

- Puente XS, Sanchez LM, Overall CM, Lopez-Otin C. (2003) Human and mouse proteases: a comparative genomic approach. *Nat. Rev. Genet.* 4:544–58.
- Gadek JD, Pacht ER. (1990) The protease-antiprotease balance within the human lung. *Lung.* 168(Suppl):552–64.
- Stoller J, Aboussouan L. (2005) Alpha1-antitrypsin deficiency. *Lancet.* 365:2225–36.
- Finlay GA, et al. (1997) Elevated levels of matrix metalloproteinases in bronchoalveolar lavage fluid of emphysematous patients. *Thorax.* 52:502–6.
- Barnes PJ. (2000) Chronic obstructive pulmonary disease. *N. Engl. J. Med.* 343:269–80.
- Rowe SM, Miller S, Sorscher EJ. (2005) Cystic fibrosis. *N. Engl. J. Med.* 352:1992–2001.
- Birrer P, et al. (1994) Protease-antiprotease imbalance in the lungs of children with cystic fibrosis. *Am. J. Respir. Crit. Care Med.* 150:207–13.
- Doring G. (1994) The role of neutrophil elastase in chronic inflammation. *Am. J. Respir. Crit. Care Med.* 150:S114–7.
- Ordonez C, et al. (2003) Inflammatory and microbiologic markers in induced sputum after intravenous antibiotics in cystic fibrosis. *Am. J. of Resp. and Crit. Care Med.* 168:1471–5.
- Walsh DE, et al. (2001) Interleukin-8 up-regulation by neutrophil elastase is mediated by MyD88/IRAK/TRAF-6 in human bronchial epithelium. *J. Biol. Chem.* 276:35494–9.
- Vandivier RW, et al. (2002) Elastase-mediated phosphatidylserine receptor cleavage impairs apoptotic cell clearance in cystic fibrosis and bronchiectasis. *J. Clin. Invest.* 109:661–70.
- Tosi MF, Zakem H, Berger M. (1990) Neutrophil elastase cleaves C3bi on opsonized *Pseudomonas* as well as CR1 on neutrophils to create a functionally important opsonin receptor mismatch. *J. Clin. Invest.* 86:300–8.
- Greenlee K, Werb Z, Kheradmand F. (2007) Matrix metalloproteinases in lung: multiple, multifarious, and multifaceted. *Physiol. Rev.* 87:69–98.
- Stamenkovic I. (2003) Extracellular matrix remodelling: the role of matrix metalloproteinases. *J. Pathology.* 200:448–64.
- Sternlicht MD, Werb Z. (2001) How matrix metalloproteinases regulate cell behavior. *Annu. Rev. Cell Dev. Biol.* 17:463–516.
- Gaggar A, et al. (2008) A novel proteolytic cascade generates an extracellular matrix-derived chemoattractant in chronic neutrophilic inflammation. *J. Immunol.* 180:5662–9.
- Triebel S, Blaser J, Reinke H, Knauper V, Tschesche H. (1992) Mercurial activation of human PMN leucocyte type IV procollagenase (gelatinase). *FEBS Lett.* 298:280–4.
- Sorsa T, et al. (1997) Activation of type IV procollagenases by human tumor-associated trypsin-2. *J. Biol. Chem.* 272:21067–74.
- Van den Steen PE, et al. (2002) Biochemistry and molecular biology of gelatinase B or matrix metalloproteinase-9 (MMP-9). *Crit. Rev. Biochem. Mol. Biol.* 37:375–536.
- Jones JL, Glynn P, Walker RA. (1999) Expression of MMP-2 and MMP-9, their inhibitors, and the activator MT1-MMP in primary breast carcinomas. *J. Pathol.* 189:161–8.
- Shapiro SD, Senior RM. (1999) Matrix metalloproteinases: matrix degradation and more. *Am. J. Respir. Cell Mol. Biol.* 20:1100–2.
- Finlay GA, et al. (1997) Matrix metalloproteinase expression and production by alveolar macrophages in emphysema. *Thorax.* 52:502–6.
- Tanaka H, et al. (2000) Sputum matrix metalloproteinase-9: tissue inhibitor of metalloproteinase-1 ratio in acute asthma. *J. Allerg. Clin. Immunol.* 105:900–5.
- Gaggar A, et al. (2007) Matrix metalloproteinase-9 dysregulation in lower airway secretions of cystic fibrosis patients. *Am. J. Physiol. Lung Cell. Mol. Physiol.* 293:L96–104.
- Okada Y, et al. (1988) Inactivation of tissue inhibitor of metalloproteinases by neutrophil elastase and other serine proteinases. *FEBS Lett.* 229:157–60.
- Nagase H, Suzuki K, Cawston TE, Brew K. (1997) Involvement of a region near valine-69 of tissue inhibitor of metalloproteinases (TIMP)-1 in the interaction with matrix metalloproteinase 3 (stromelysin 1). *Biochem. J.* 325:163–7.
- Ferry G, et al. (1997) Activation of MMP-9 by neutrophil elastase in an in vivo model of acute lung injury. *FEBS Lett.* 402:111–5.
- Hilliard JB, Konstan MW, Davis PB. (2002) Inflammatory mediators in CF patients. *Methods Mol. Med.* 70:409–31.
- Geraghty P, et al. (2007) Neutrophil elastase up-regulates cathepsin B and matrix metalloproteinase-2 expression. *J. Immunol.* 178:5871–8.
- Bieth JG. (1986) Elastases: catalytic and biological properties. In: *Regulation of Matrix Accumulation*. RP Mecham (ed.) Academic Press, Orlando (FL), pp. 217–30.
- Lee ER, Lamplugh L, Kluczyk B, Mort JS, Leblond CP. (2006) Protease analysis by neopeptide approach reveals the activation of MMP-9 is achieved proteolytically in a test tissue cartilage model involved in bone formation. *J. Histochem. Cytochem.* 54:965–80.
- Springman EB, Angleton EL, Birkedal-Hansen H, Van Wart HE. (1990) Multiple modes of activation of latent human fibroblast collagenase: evidence for the role of a Cys73 active-site zinc complex in latency and a “cysteine switch” mechanism for activation. *PNAS.* 87:364–8.
- Nagase H, Brew K. (2002) Engineering of tissue inhibitor of metalloproteinases mutants as potential therapeutics. *Arthritis Res.* 4(Suppl 3):S51–61.